Mobile Impulse Response Generator (MIRG):
A Geometric Optics Model

Michael G. Cotton
U.S. Department of Commerce
National Telecommunications and Information Administration
Institute for Telecommunication Sciences
325 Broadway
Boulder, Colorado 80303 USA
Telephone: (303)497-7346
Fax: (303)497-3680
email: mcotton@ntia.its.bldrdoc.gov

1. Introduction

The objective of this research is to derive a theoretical description of an indoor channel based on specular reflections. The Mobile Impulse Response Generator (MIRG) calculates the impulse response of an indoor channel, geometrically defined as a cuboid with no openings or obstructions (no windows, doors, or objects within the room). The receiver or transmitter may move about the room, hence, providing the model with a mobility parameter. A recursive imaging algorithm is utilized to compute all possible rays with up to twenty bounces. Moreover, the free space loss and polarization dependent complex reflection coefficients are computed to define the amplitude and phase change of each ray. This paper will not attempt to explain the physics of the mobile indoor channel, however, it will define the parameters of the MIRG program, list all assumptions, and give a simple example.

2. Summary of MIRG

MIRG is an efficient ray tracing model which utilizes a recursive imaging algorithm to find all possible paths with up to 20 bounces. Typically, theoretical impulse responses considering up to five reflections is a sufficient description for an indoor channel; the 20-bounce ability allows for the study of special cases, such as: metallic rooms and anechoic chambers at frequencies below 80-MHz [3]. The model assumes smooth wall, ceiling, and floor surfaces, and the room is taken as a perfect cuboid with no objects within.

The model follows a systematic algorithm in calculating the requested data. The user selects the mobile path for the transmitter or receiver. For each position of the mobile node MIRG proceeds to find all possible combinations of bounces which result in a ray adhering to classic Fresnel reflections [4]. Once a feasible path is found, it is necessary for MIRG to convert the user-defined polarization from the horizontal-vertical reference frame to the frame of reference corresponding to the plane of incidence. Next the electric field is decoupled into orthogonal components, hence defining the parallel and perpendicular components relative to the first surface. Complex Fresnel reflection coefficients are defined and the reflected electric field vector

is derived from the existing boundary conditions. The routine continues through the predetermined sequence of reflections reiterating this procedure. Lastly, the attenuation and phase change due to free space is incorporated.

The impulse responses can be written in two output formats: 1) an ascii text file containing a header with the user-defined model parameters and the calculated total energy received; alternatively, 2) the impulse responses may be converted into a binary FIR filter file for simulation purposes.

To demonstrate flexibility of the model, a list of the MIRG input parameters is provided:

> 1. dimensions of cuboid room
> 2. initial position of transmitter
> 3. initial position of receiver
> 4. type of path, either straight, circular, or random
> 5. mobile selection of R_x or T_x
> 6. number of steps in path
> 7. maximum delay spread
> 8. number of samples in impulse response
> 9. maximum number of bounces
> 10. polarization ($p=|E_h|/|E_v|$)
> 11. wavelength (λ)
> 12. conductivity of wall (σ)
> 13. relative dielectric constant of wall (ϵ_r)

Parameters 4-6 define the path of the mobile node, hence, allowing for the generation of a mobile impulse response at unlimited spatial resolution. The sampling information defines time resolution of a FIR filter file; if the FIR time resolution is too course a number of multipath components of various path delays may contribute to the data in a single time bin, hence, obscuring the true theoretical behavior of the impulse response.

3. Case Study

Figures 1-2 in the Appendix are 3-dimensional plots of the impulse responses for 20 transmitter positions along a 1 [m] path (#1 in figure 5) with the receiver stationed in the center of the room (R_{X1}). High spatial resolution over the short path, 4 [impulses/λ], produces a more detailed portrayal of the indoor channel. Figure 3-4 demonstrate a low spatial resolution case, 0.1131 [impulse/λ], where the receiver is located in the corner and the transmitter follows a symmetric 35.4 [m] path (#2) across the room. Notice the spatial symmetry. Two initial polarizations are shown for each case: horizontal linear and vertical linear.

A 2-bounce ray from the vertically polarized, high spatial resolution case is explicitly calculated below. Table 1 is a standard ascii output of MIRG containing the calculated ray (highlighted by ****) and the geometry is visualized in figure 5 by a dashed line. For this study the table displays a stationary receiver and transmitter (Tx step: 0 of 0) and a maximum number of bounces of two. The transmitter launches an

electric field with a magnitude of $E = 1$ [V/m] and an initial phase of 0 [rad]. The multipath data computed is path delay, magnitude of the electric field, relative strength of the component normalized to the total energy received, length of ray path, and phase change.

Given the initial conditions the transmitted E field can be described as

$$\mathbf{E}_h = 0 \text{ [V/m]} \qquad \mathbf{E}_v = 1 \text{ [V/m]} \qquad \angle E_h = \angle E_v = 0 \text{ [rad]}$$

The ray under consideration propagates from the transmitter, $T_x = (2, 12.5, 2)$ [m], bounces off the reflection points, $r_1 = (7.25, 0, 8.5)$ and $r_2 = (8.462, 2.885, 10)$, and arrives at the receiver, $R_x = (12.5, 12.5, 5)$. From these points the direction of propagation from T_x to r_1 is a_1 and the horizontal and vertical polarization direction vectors are given by a_h and a_v and are shown as:

$$a_1 = 0.3492i - 0.8314j + 0.4323k$$
$$a_h = a_1 \times k = -0.9220i - 0.3872j$$
$$a_v = a_h \times a_1 = -0.1674i + 0.3986j + 0.9017k$$

where k is the vertical direction vector. The normal to the first reflection surface, $n_1 = j$, is used to decompose the E field into a complex representation of the parallel and perpendicular components relative to the plane of incidence.

$$a_{\perp 1} = a_1 \times n_1 = -0.7779i + 0.6283k$$
$$\text{Real}(E_{\perp 1}) = \mathbf{E}_h | a_{\perp 1} \cdot a_h | \cos\angle E_h + \mathbf{E}_v | a_{\perp 1} \cdot a_v | \cos\angle E_v = 0.6968$$
$$\text{Imag}(E_{\perp 1}) = \mathbf{E}_h | a_{\perp 1} \cdot a_h | \sin\angle E_h + \mathbf{E}_v | a_{\perp 1} \cdot a_v | \sin\angle E_v = 0$$

$$a_{\parallel 1} = a_{\perp 1} \times a_1 = 0.5224i + 0.5557j + 0.6468k$$
$$\text{Real}(E_{\parallel 1}) = \mathbf{E}_h | a_{\parallel 1} \cdot a_h | \cos\angle E_h + \mathbf{E}_v | a_{\parallel 1} \cdot a_v | \cos\angle E_v = 0.7172$$
$$\text{Imag}(E_{\parallel 1}) = \mathbf{E}_h | a_{\parallel 1} \cdot a_h | \sin\angle E_h + \mathbf{E}_v | a_{\parallel 1} \cdot a_v | \sin\angle E_v = 0$$

The angle of incidence, $\phi_1 = 0.5892$ [rad], and polarization dependent, complex Fresnel reflection coefficients, $\Gamma_{\parallel}(\phi_1, \epsilon_r, \sigma, \lambda)$ and $\Gamma_{\perp}(\phi_1, \epsilon_r, \sigma, \lambda)$, are derived from the geometry and the user defined specifications. The tangential component of an E field is continuous at an interface. This boundary condition dictates the orientation of the E field after the reflection.

$$a_{\perp 1} = 0.7779i - 0.6283k$$
$$E_{\perp 2} = E_{\perp 1}\Gamma_{\perp 1} = 0.2590 - i0.0005$$

$$a_{\parallel 1} = -0.5224i + 0.5557j - 0.6468k$$
$$E_{\parallel 2} = E_{\parallel 1}\Gamma_{\parallel 1} = -0.3595 + i0.0005$$

Using similar arguments, the E field is decoupled into parallel and perpendicular components relative to the

second plane of incidence and respective reflection coefficients are applied. After two reflections all bounces have been accounted for, hence, the resulting electric field, E_3, describes the accumulative attenuation and phase change due to the specular reflections.

$$E_{\perp3} = 0.0055 \text{ [V/m]} \quad \angle E_{\perp3} = 3.133 \text{ [rad]}$$

$$E_{|3} = 0.0538 \text{ [V/m]} \quad \angle E_{|3} = -0.0008 \text{ [rad]}$$

Lastly, the free space loss contribution is computed over the entire path, d=30.07 [m].

$$a = (\lambda/4\pi d)^2 = 2.797 \times 10^{-7} \quad \beta_0 d = (2\pi d)/\lambda = 2.877 \text{ rad}$$

$$E = a(E_{\perp3}^2 + E_{\perp3}^2)^{\frac{1}{2}} = 1.512 \times 10^{-8} \text{ [V]} \quad \angle E = \angle E_{\perp3} + \angle E_{|3} - \beta_0 d = 0.2553 \text{ [rad]}$$

4. Conclusion

MIRG computes the theoretical impulse response of a mobile indoor channel at high spatial resolution. A systematic approach to the problem allows for the future expansion of the model into different scenarios, such as;

1. arbitrary mobile paths
2. antenna patterns
3. incorporating objects into the room
4. different shapes of rooms (ie. doors, windows, circular room)
5. rays switched on/off at varying rates to simulate the effect of rotating machinery
6. application to anechoic chambers
7. application to urban environments

The model is idealistic and outputs information resulting from the specular reflections and free space loss in the room. It provides an efficient means of obtaining the parameters essential to the design and modeling of indoor communication systems.

5. Appendix

PHYSICAL PARAMETERS:
Room dimensions [m]: X= 25.0, Y= 25.0, Z= 10.0
Transmitter [m]:   Tx= 2.0, Ty= 12.5, Tz= 2.0
Receiver [m]:   Rx= 12.5, Ry= 12.5, Rz= 5.0
Tx step: 0 of 0
Sampling info.:   T=1.270000e-006 sec SR=6.795276e+008 sample/sec

WAVE PROPERTIES:
Wavelength: lambda= 0.200 m (f=1500.000 MHz)
Polarization: p=0.000

CHANNEL CHARACTERISTICS:
Wall conductivity: sigma= 0.001950 mho/m
Rel. dielectric: er= 6.5700
Maximum bounces: max_b= 2
Total Energy: E= 0.0062E-9 J

MULTIPATH COMPONENTS:

Delay[nsec]	Mag[mV]	RStngth[V]	d[m]	Phase[rad]
0.0364	0.0021	0.8490	10.9202	2.2706
0.0494	0.0005	0.2059	14.8071	2.5951
0.1321	0.0000	0.0125	39.6138	4.9861
0.0969	0.0000	0.0064	29.0560	3.9378
0.0969	0.0000	0.0064	29.0560	3.9378
0.0537	0.0003	0.1284	16.1012	2.7501
0.0650	0.0002	0.0821	19.4743	3.5217
0.1188	0.0001	0.0351	35.6265	1.5315
0.2021	0.0000	0.0053	60.5743	5.7688
0.0910	0.0001	0.0561	27.2809	0.0020
0.1452	0.0000	0.0041	43.5230	4.5657
0.1707	0.0000	0.0072	51.1786	5.8356
0.1003	0.0000	0.0061	30.0707	0.2553****
0.0910	0.0001	0.0561	27.2809	0.0020
0.1452	0.0000	0.0041	43.5230	4.5657
0.1707	0.0000	0.0072	51.1786	5.8356
0.1003	0.0000	0.0061	30.0707	0.2553
0.0421	0.0010	0.3990	12.6194	2.2558
0.1207	0.0001	0.0292	36.1836	6.0108
0.0934	0.0001	0.0439	28.0045	2.3881
0.0934	0.0001	0.0439	28.0045	2.3881
0.0667	0.0002	0.0618	19.9812	0.1519
0.0557	0.0005	0.1897	16.7108	5.5799
0.1261	0.0001	0.0244	37.8054	5.2884
0.0843	0.0001	0.0351	25.2834	3.1104

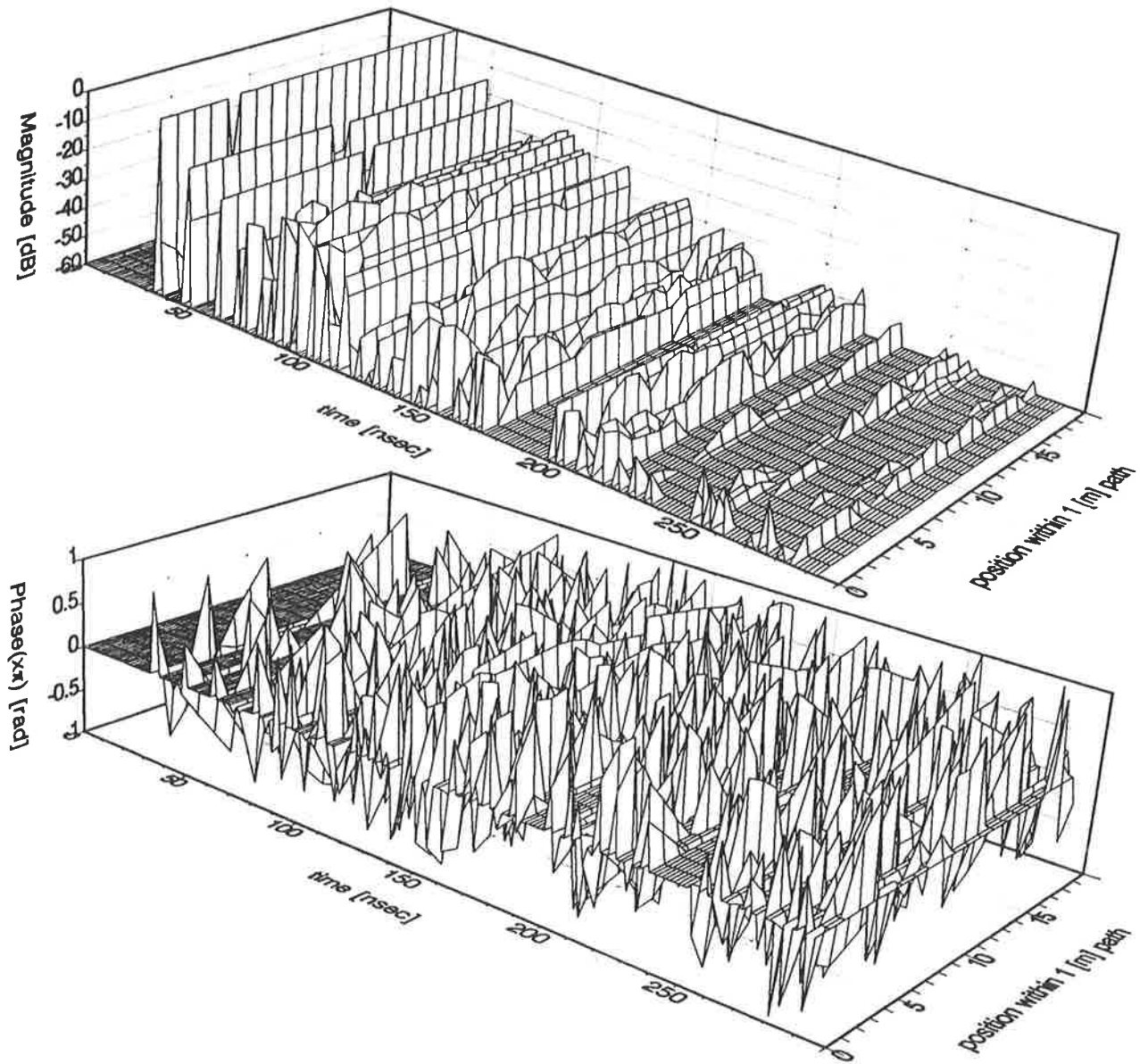**Table 1.** Single-Position Impulse Response Output of MIRG

Figure 1. Calculated mobile indoor channel impulse response (horizontal linear polarization) showing (top) magnitude and (bottom) phase: mobile T_x (20 steps along 1[m] path #1); receiver stationed in center of 25×25×10 [m] room.
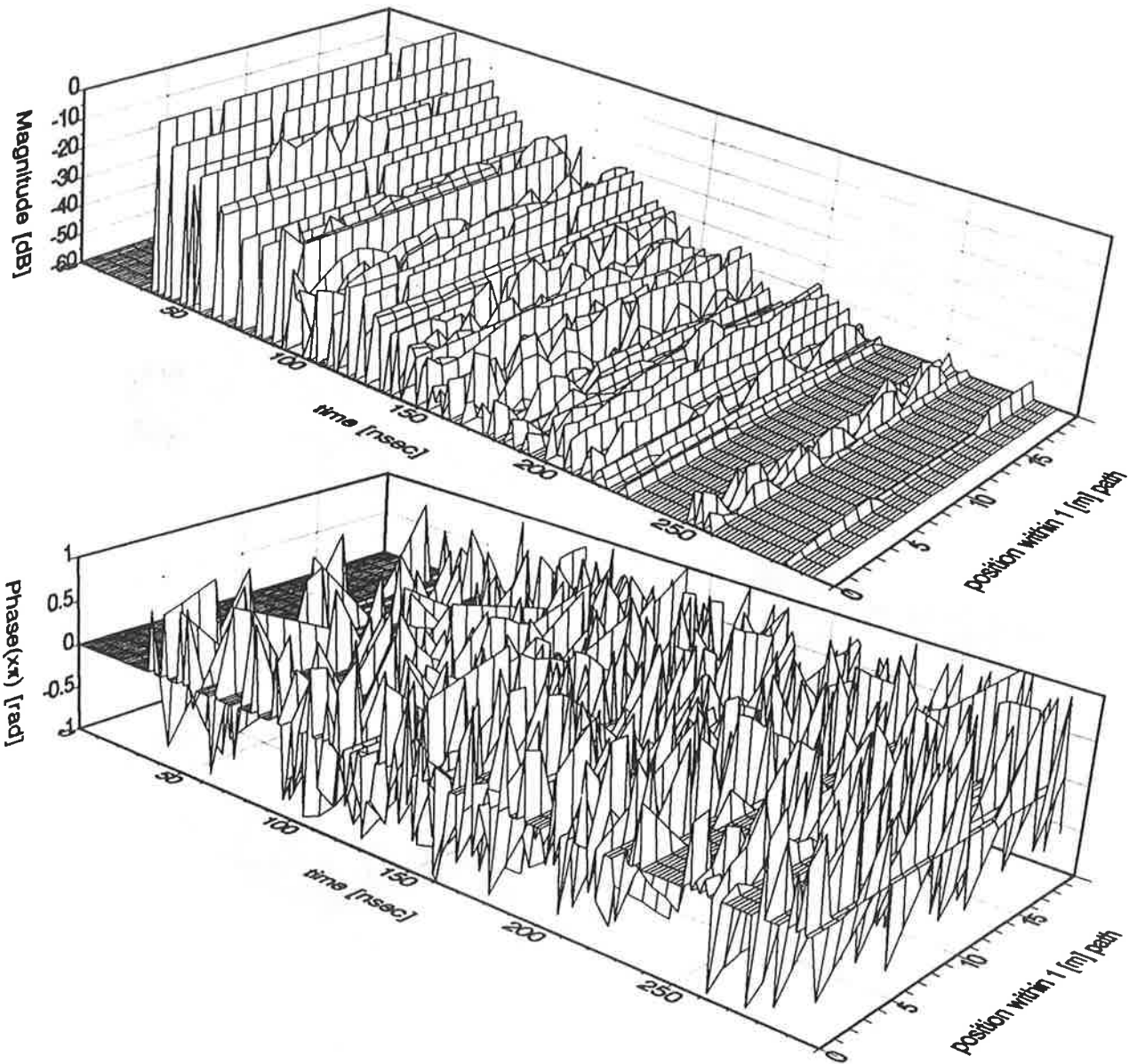
Figure 2. Calculated mobile indoor channel impulse response (vertical linear polarization) showing (top) magnitude and (bottom) phase: mobile T_x (20 steps along 1[m] path #1); receiver stationed in center of $25 \times 25 \times 10$ [m] room.
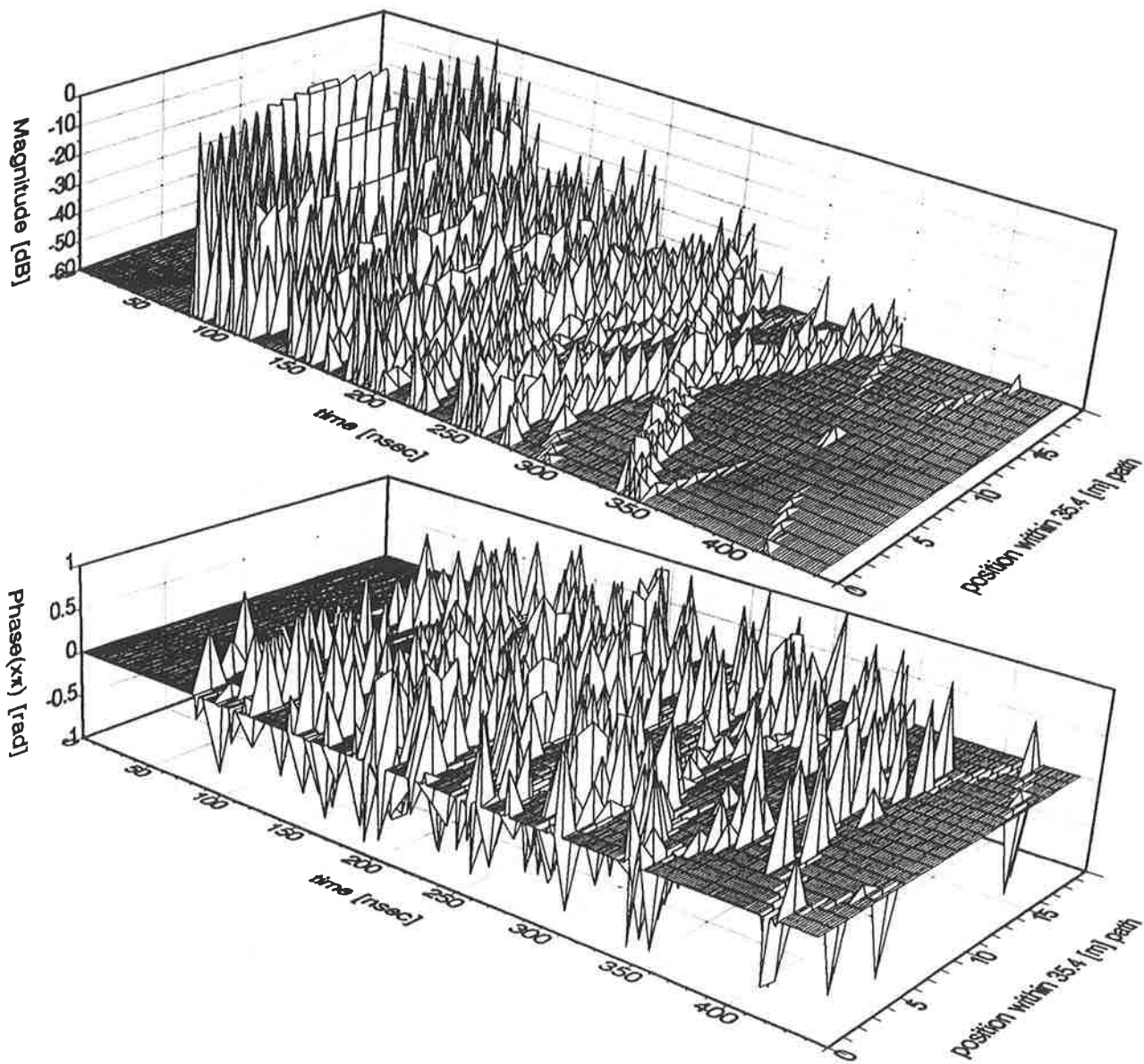
Figure 3.   Calculated mobile indoor channel impulse response (horizontal linear polarization) showing (top) magnitude and (bottom) phase: mobile T_x (20 steps along 35.4[m] path #2); receiver stationed in corner of 25×25×10 [m] room.
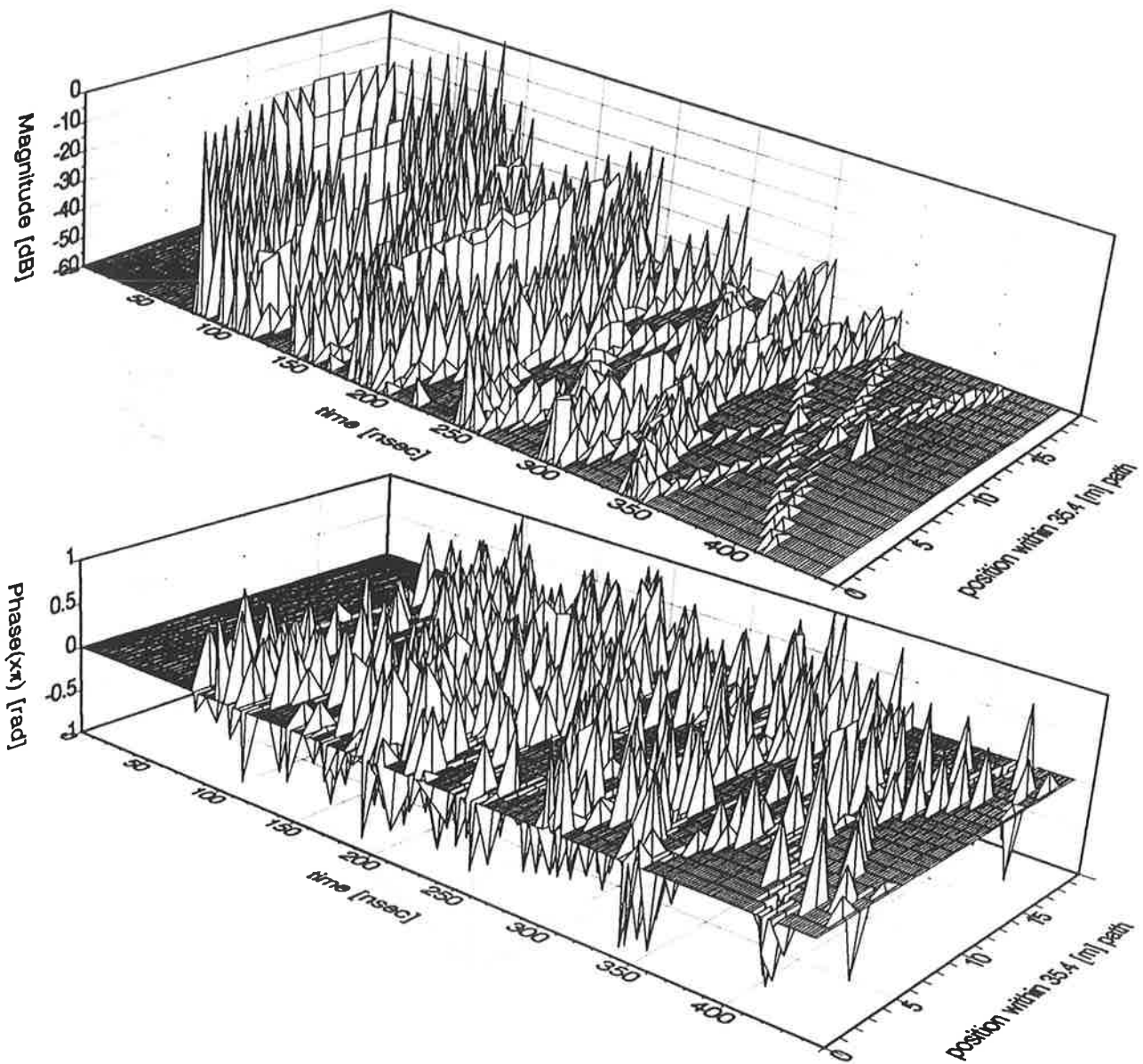
Figure 4.   Calculated mobile indoor channel impulse response (vertical linear polarization) showing (top) magnitude and (bottom) phase: mobile T_x (20 steps along 35.4[m] path #2); receiver stationed in corner of $25 \times 25 \times 10$ [m] room.
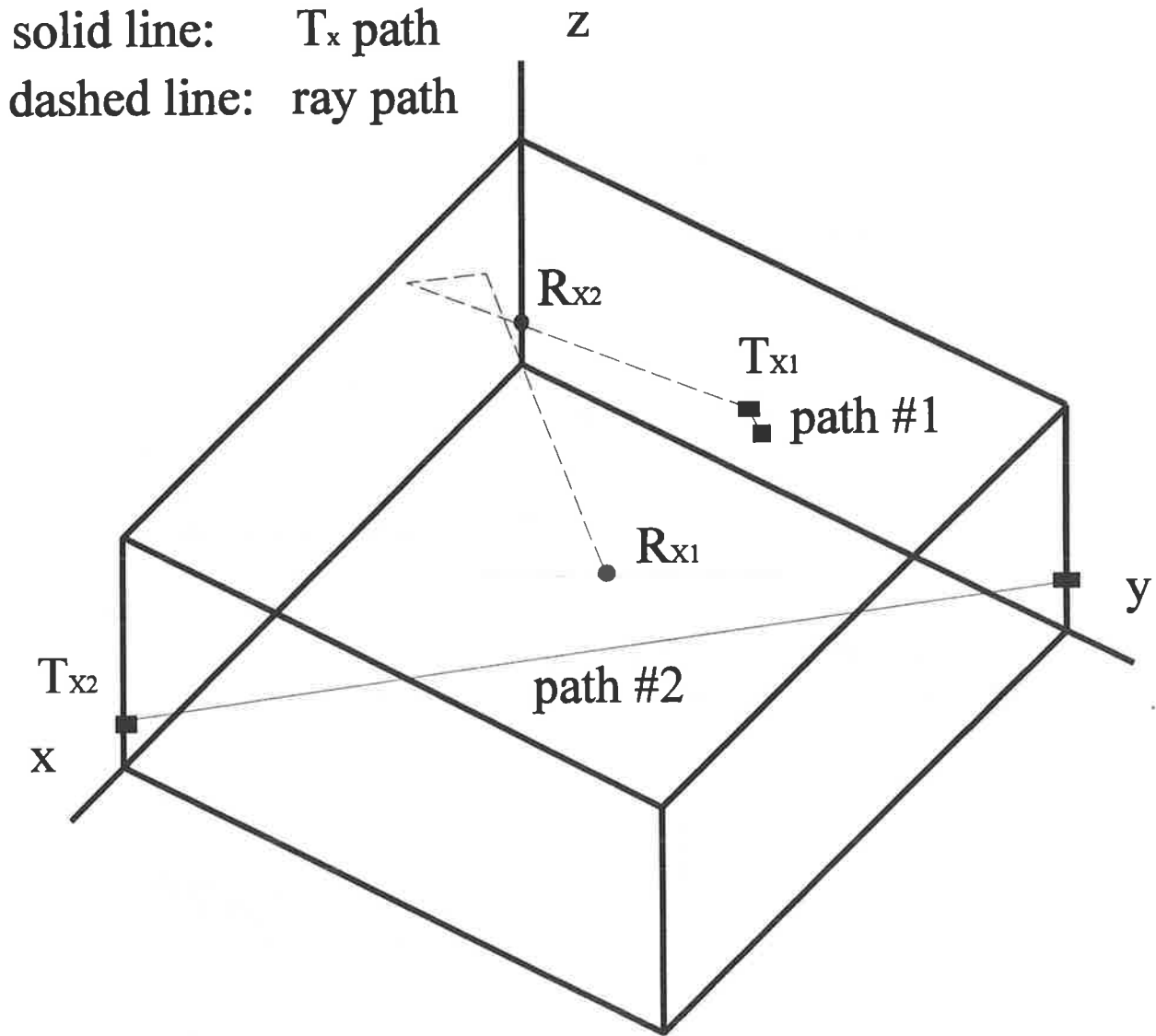
solid line: T$_x$ path
dashed line: ray path

Figure 5.   Geometry of Indoor Channel

5. References

[1]   Achatz, R.J., "Geometric Optics Indoor Channel Model", IEEE P802.11-94/261, November 1994.

[2]   Allen, K.A., "A Model of Millimeter-Wave Propagation for Personal Communication Networks in Urban Settings", NTIA Report 91-275, April 1991.

[3]   Holloway, C.L. and Kuester, E.F., "Modeling Semi-Anechoic Electromagnetic Measurement Chambers", submitted to IEEE Trans. on EMC, 1994.

[4]   Johnk, C.A. (1988), "Engineering Electromagnetic Fields and Waves", John Wiley and Sons, New York.